Scattering by a Cavity in an Exponentially Graded Half-Space

P. A. Martin
Department of Mathematical and Computer Sciences,
Colorado School of Mines,
Golden, CO 80401-1887
e-mail: pamartin@mines.edu

An inhomogeneous half-space containing a cavity is bonded to a homogeneous half-space. Waves are incident on the interface and the problem is to calculate the scattered waves. For a circular cavity in an exponentially graded half-space, it is shown how to solve the problem by constructing an appropriate set of multipole functions. These functions are singular on the axis of the cavity, they satisfy the governing differential equation in each half-space, and they satisfy the continuity conditions across the interface between the two half-spaces. Seven recent publications are criticized: They do not take proper account of the interface between the two half-spaces. [DOI: 10.1115/1.3086585]

1 Introduction

Consider two half-spaces, $x>0$ and $x<0$, welded together along the interface at $x=0$. The left half-space ($x<0$) is homogeneous. The right half-space is inhomogeneous. If a wave is incident from the left, it will be partly reflected and partly transmitted into the right half-space. We assume that these fields can be calculated.

Suppose now that the right half-space contains a cavity or some other defect (see Fig. 1). How are the basic fields described above modified by the presence of the cavity? In general, it is not easy to answer this question, as the associated mathematical problem is difficult, in general.

In some recent papers, Fang et al. claimed to solve a variety of such problems. All concern "exponential grading," meaning that the material parameters are proportional to $e^{-\beta x}$ for $x>0$, where β is a given constant. The papers concern antiplane shear waves [1–4], thermal waves [5,6], and shear waves in a piezoelectric material [7]. All of these papers assume that the effect of the interface on the cavity can be found by introducing simple image terms, as if the interface were a mirror or a rigid wall. Unfortunately, this assumption is incorrect.

In this paper, we outline how the problems described above can be solved. We do this in the context of antiplane shear waves with exponential grading and a circular cavity. The main technical part concerns the derivation of suitable multipole potentials; these reveal the complicated image system.

The study of problems involving scatterers near boundaries or interfaces has a long history. For linear surface water waves interacting with a submerged circular cylinder, see the famous paper by Ursell [8]. For plane-strain elastic waves in a homogeneous half-space with a buried circular cavity, see Ref. [9]. There are also many papers on the scattering of electromagnetic waves by objects near plane boundaries; see, for example, Ref. [10].

Some problems involving objects near plane boundaries can be solved using images. However, determining the strength and location of the images may be difficult: Doing so will depend on the governing differential equations and on the conditions to be satisfied on the plane boundary. For two interesting examples where the location of the images is not obvious, we refer to Chap. 8 of Ting's book [11] (construction of static Green's functions in anisotropic elasticity) and a paper by Stevenson [12] (construction of Green's function for the anisotropic Helmholtz equation in a half-space).

The basic scattering problem is formulated in Sec. 2. The reflection-transmission problem (for which the cavity is absent) is solved in Sec. 3. The solution of this problem gives the "incident" field that will be scattered by the cavity. To solve the scattering problem, we construct an appropriate set of multipole functions (Sec. 4.1). Each of these satisfies the governing differential equations and the interface conditions, and is singular at the center of the circular cavity. Each multipole function is defined as a contour integral of Sommerfeld type; for a careful discussion of similar functions, see Refs. [13,9]. In Sec. 4.2, the multipole functions are combined so as to satisfy the boundary condition on the cavity, leading to an infinite linear system of algebraic equations. The far-field behavior of the multipole functions is deduced in Sec. 4.3. Closing remarks are made in Sec. 5.

2 Formulation

We consider the antiplane deformations of two elastic half-spaces, bonded together. In terms of Cartesian coordinates (x,y), the half-space $x<0$ is homogeneous, the half-space $x>0$ is inhomogeneous ("graded"), and the interface is at $x=0$. The homogeneous region has shear modulus μ_0 and density ρ_0 (both constants). The inhomogeneous region has shear modulus $\mu(x)$ and density $\rho(x)$ given by

$$\mu(x)=\mu_0 e^{2\beta x} \quad \text{and} \quad \rho(x)=\rho_0 e^{2\beta x} \tag{1}$$

where β is a constant. Thus, the material parameters are continuous across the interface.

It is not our purpose here to discuss whether any real materials can be well represented by the functional forms given in Eq. (1). Certainly, the choices in Eq. (1) do lead to some mathematical simplifications and they have been used in the past; see, for example, Refs. [14,15].

For time-harmonic motions, with suppressed time-dependence $e^{-i\omega t}$, the governing equation is

$$\frac{\partial \tau_{xz}}{\partial x}+\frac{\partial \tau_{yz}}{\partial y}+u\omega^2\rho(x)=0$$

where $u(x,y)$ is the antiplane component of displacement and the stress components are given by

$$\tau_{xz}=\mu(x)\frac{\partial u}{\partial x} \quad \text{and} \quad \tau_{yz}=\mu(x)\frac{\partial u}{\partial y}$$

Thus, in the homogeneous region, where we write u_0 instead of u, we obtain the two-dimensional Helmholtz equation

$$(\nabla^2+k_0^2)u_0=0 \quad \text{with} \quad k_0^2=\rho_0\omega_2/\mu_0 \tag{2}$$

In the inhomogeneous region, we obtain

$$\nabla^2 u+2\beta\frac{\partial u}{\partial x}+k_0^2 u=0$$

This equation is satisfied by writing

Contributed by the Applied Mechanics Division of ASME for publication in the Journal of Applied Mechanics. Manuscript received November 12, 2007; final manuscript received March 10, 2008; published online March 10, 2009. Review conducted by Professor Sridhar Krishnaswamy.

Downloaded 13 Mar 2009 to 138.67.22.171. Redistribution subject to ASME license or copyright; see http://www.asme.org/terms/Terms_Use.cfm

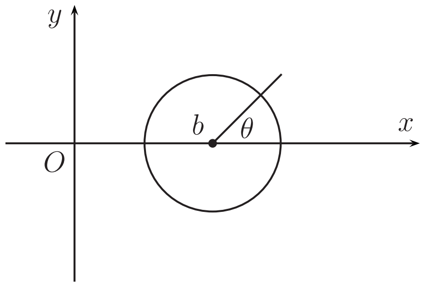

Fig. 1 The scattering problem. The half-plane on the left of $x=0$ is homogeneous. The other half-plane is inhomogeneous. The circular cavity has radius a. A plane wave is incident from the left.

$$u(x,y)=e^{-\beta x}w(x,y)$$

where w satisfies a different two-dimensional Helmholtz equation

$$(\nabla^2+k^2)w=0 \quad \text{with} \quad k^2=k_0^2-\beta^2 \tag{3}$$

For simplicity, we assume that $k_0^2>\beta^2$ and write $k=+\sqrt{k_0^2-\beta^2}$.

The interface conditions require that the displacements and normal stresses be continuous, so that

$$u_0(0,y)=u(0,y)=w(0,y) \tag{4}$$

$$\left.\frac{\partial u_0}{\partial x}\right|_{x=0}=\left.\frac{\partial u}{\partial x}\right|_{x=0}=\left.\frac{\partial w}{\partial x}\right|_{x=0}-\beta w(0,y) \tag{5}$$

3 Incident Field

Suppose that a plane wave is incident on the interface from the homogeneous side. This wave is given by

$$u_{\text{in}}(x,y)=e^{ik_0(x\cos\alpha_0+y\sin\alpha_0)}$$

where α_0 is the angle of incidence, $|\alpha_0|<\pi/2$; $\alpha_0=0$ gives normal incidence. There will be a reflected wave u_{re} and a transmitted wave u_{tr}. Evidently,

$$u_{\text{re}}(x,y)=\mathcal{R}e^{ik_0(-x\cos\alpha_0+y\sin\alpha_0)}, \quad x<0 \tag{6}$$

$$u_{\text{tr}}(x,y)=\mathcal{T}e^{-\beta x}e^{ik(x\cos\alpha+y\sin\alpha)}, \quad x>0 \tag{7}$$

where $\mathcal{R}$, $\mathcal{T}$, and α are to be found. Writing $u_0=u_{\text{in}}+u_{\text{re}}$ and $u=u_{\text{tr}}$, Eq. (4) gives

$$1+\mathcal{R}=\mathcal{T} \quad \text{and} \quad k_0\sin\alpha_0=k\sin\alpha$$

Then, Eq. (5) gives

$$(1-\mathcal{R})ik_0\cos\alpha_0=\mathcal{T}(ik\cos\alpha-\beta)$$

Solving for $\mathcal{R}$ gives

$$\mathcal{R}=\frac{k_0\cos\alpha_0-k\cos\alpha-i\beta}{k_0\cos\alpha_0+k\cos\alpha+i\beta}=\frac{-i\beta}{k_0\cos\alpha_0+k\cos\alpha}$$

and then $\mathcal{T}=1+\mathcal{R}$.

For a simple check, put $\beta=0$; we obtain $k=k_0$, $\alpha=\alpha_0$, $\mathcal{R}=0$, and $\mathcal{T}=1$, as expected.

4 Scattering by a Buried Cavity

Next, we investigate how the wavefields of Sec. 3 are modified if there is a cavity in the inhomogeneous half-space, $x>0$. See Fig. 1.

We suppose that the cavity's cross section is circular, with boundary

$$(x-b)^2+y^2=a^2 \quad \text{with} \quad 0<a<b$$

We also introduce polar coordinates, (r,θ), so that

$$x=b+r\cos\theta \quad \text{and} \quad y=r\sin\theta \tag{8}$$

Thus, the cavity's boundary is given by $r=a$, and the boundary condition is

$$\frac{\partial u}{\partial r}=0 \quad \text{on} \quad r=a \tag{9}$$

where u is the total field in the inhomogeneous half-space.

To solve such a scattering problem, we write

$$u_0=u_{\text{in}}+u_{\text{re}}+v_0, \quad x<0$$

$$u=u_{\text{tr}}+v, \quad x>0, \quad r>a$$

where v_0 solves Eq. (2), $v=we^{-\beta x}$, and w solves Eq. (3). Also, v_0 must satisfy the Sommerfeld radiation condition and v must decay with x.

4.1 Multipole Functions.

To represent the scattered field, we introduce functions ϕ_n of the form

$$\phi_n=\begin{cases} e^{-\beta x}\{H_n^{(1)}(kr)e^{in\theta}+\Phi_n\}, & x>0 \\ \Psi_n, & x<0 \end{cases}$$

where $H_n^{(1)}$ is a Hankel function and n is an arbitrary integer. We require that Φ_n solves Eq. (3) and Ψ_n solves Eq. (2). In addition, Φ_n and Ψ_n are to be chosen so that ϕ_n satisfies the interface conditions, Eqs. (4) and (5).

The use of polar coordinates is convenient for handling the circular cavity but it is inconvenient when trying to impose the conditions at $x=0$. Therefore, we convert from polar coordinates to Cartesian coordinates using an integral representation; see the Appendix for details. In particular, if we insert Eq. (8) in Eq. (A4), we obtain the integral representation

$$H_n^{(1)}(kr)e^{in\theta}=\frac{(-1)^n}{\pi i}\int_{-\infty}^{\infty+\pi i}e^{k(b-x)\sinh\tau-iky\cosh\tau}e^{-n\tau}\mathrm{d}\tau$$

$$\text{for} \quad x<b, |y|<\infty \tag{10}$$

Notice that this formula is valid on the interface $x=0$. The contour of integration in Eq. (10) is also described in the Appendix.

The form of Eq. (10) suggests using a similar integral representation for Φ_n, and so we write

$$\Phi_n(x,y)=\frac{(-1)^n}{\pi i}\int_{-\infty}^{\infty+\pi i}A(\tau)e^{kx\sinh\tau}e^{-iky\cosh\tau+kb\sinh\tau-n\tau}\mathrm{d}\tau, \quad x>0 \tag{11}$$

where $A(\tau)$ is to be found; Φ_n solves Eq. (3) automatically for any reasonable choice of A.

We shall also need a similar integral representation for $\Psi_n(x,y)$ in $x<0$, where the wavenumber is k_0. However, in order to match solutions across the interface at $x=0$, we shall require the same dependence on y as in Eq. (11). Thus, we consider

$$\Psi_n(x,y)=\frac{(-1)^n}{\pi i}\int_{-\infty}^{\infty+\pi i}B(\tau)e^{x\Delta(\tau)}e^{-iky\cosh\tau+kb\sinh\tau-n\tau}\mathrm{d}\tau, \quad x<0 \tag{12}$$

where $B(\tau)$ is to be found,

$$\Delta(\tau)=(k^2\cosh^2\tau-k_0^2)^{1/2}=(k^2\sinh^2\tau-\beta^2)^{1/2}$$

and the square root is taken so that $\operatorname{Re}\Delta\geq 0$ on the contour. Notice that Eq. (2) is satisfied automatically for any reasonable choice of B.

We are now ready to enforce the interface conditions. Continuity of ϕ_n across $x=0$ gives $1+A=B$ whereas continuity of $\partial\phi_n/\partial x$ gives

Downloaded 13 Mar 2009 to 138.67.22.171. Redistribution subject to ASME license or copyright; see http://www.asme.org/terms/Terms_Use.cfm

$$-k \sinh \tau - \beta + (k \sinh \tau - \beta) A(\tau) = \Delta(\tau) B(\tau)$$

Hence

$$A(\tau) = \frac{k \sinh \tau + \Delta + \beta}{k \sinh \tau - \Delta - \beta} \tag{13}$$

and

$$B(\tau) = \frac{2k \sinh \tau}{k \sinh \tau - \Delta - \beta} \tag{14}$$

These formulas complete the construction of the multipole functions ϕ_n.

Note that when $\beta=0$, $k=k_0$, $\Delta(\tau)=-k \sinh \tau$, $A=0$, $B=1$, and $\Psi_n = H_n^{(1)}(kr)e^{in\theta}$, as expected.

4.2 Imposing the Boundary Condition. In the homogeneous half-space, we write

$$u_0 = u_{\mathrm{in}} + u_{\mathrm{re}} + \sum_n c_n \phi_n$$

where Σ_n denotes summation over all integers n. Similarly, in the graded half-space, we write

$$u(r,\theta) = u_{\mathrm{tr}} + \sum_n c_n \phi_n$$

Then, by construction, the governing partial differential equations and the interface conditions along $x=0$ are all satisfied. It remains to determine the coefficients c_n using the boundary condition on $r=a$, Eq. (9); this gives

$$\sum_n c_n \left. \frac{\partial \phi_n}{\partial r} \right|_{r=a} = - \left. \frac{\partial u_{\mathrm{tr}}}{\partial r} \right|_{r=a} \tag{15}$$

To proceed, we write both sides of this equation as Fourier series in θ. For the right-hand side, we have

$$u_{\mathrm{tr}} = e^{-\beta x} \mathcal{T}_b e^{ikr \cos(\theta - \alpha)} = e^{-\beta x} \mathcal{T}_b \sum_m i^m J_m(kr) e^{im(\theta-\alpha)}$$

where $\mathcal{T}_b = \mathcal{T} \exp(ikb \cos \alpha)$ and J_n is a Bessel function. Also, we have the expansion

$$e^{-\beta x} = e^{-\beta b} \sum_s (-1)^s I_s(\beta r) e^{is\theta}$$

where I_n is a modified Bessel function. Hence,

$$u_{\mathrm{tr}}(r,\theta) = e^{-\beta b} \sum_m (-1)^m U_m(r) e^{im\theta}$$

where

$$U_m(r) = \mathcal{T}_b \sum_s (-i)^s I_{m-s}(\beta r) J_s(kr) e^{-is\alpha}$$

In a similar way, we obtain

$$\Phi_n(r,\theta) = \sum_m (-1)^m f_m^n J_m(kr) e^{im\theta}, \quad 0 < r < b$$

with

$$f_m^n = \frac{(-1)^n}{\pi i} \int_{-\infty}^{\infty + \pi i} A(\tau) e^{2kb \sinh \tau} e^{-(m+n)\tau} \mathrm{d}\tau$$

Hence

$$\phi_n(r,\theta) = e^{-\beta b} \sum_m (-1)^m V_m^n(r) e^{im\theta}$$

where

$$V_m^n(r) = (-1)^n I_{m-n}(\beta r) H_n^{(1)}(kr) + \sum_s f_s^n I_{m-s}(\beta r) J_s(kr) \tag{16}$$

Thus, Eq. (15) and orthogonality of $\{e^{im\theta}\}$ give

$$\sum_n c_n V_m^{n\prime}(a) = -U_m'(a), \quad \text{all} \quad m \tag{17}$$

which is a linear system of algebraic equations for the coefficients c_n.

4.3 Far-Field Behavior of Ψ_n. We should expect cylindrical waves in the homogeneous half-space. These arise from the far-field behavior of $\Psi_n(x,y)$, for $x<0$. Thus, put

$$x = -R \cos \Theta, \quad y = R \sin \Theta, \quad |\Theta| < \pi/2$$

Then, making the substitution $k \cosh \tau = k_0 \cosh s$ in Eq. (12) gives $\Delta = -k_0 \sinh s$ and

$$\Psi_n = \frac{1}{\pi i} \int_{-\infty}^{\infty + \pi i} \mathcal{B}_n(k_0 \cosh s; \beta) e^{k_0 R \sinh(s - i\Theta)} \mathrm{d}s, \quad |\Theta| < \pi/2 \tag{18}$$

where

$$\mathcal{B}_n(\zeta;\beta) = \frac{2(\zeta^2 - k_0^2)^{1/2} \exp\{-b(\zeta^2 - k^2)^{1/2}\}}{(\zeta^2 - k^2)^{1/2} + \beta + (\zeta^2 - k_0^2)^{1/2}} \left(\frac{\zeta + (\zeta^2 - k^2)^{1/2}}{(-k)} \right)^n$$

the square roots being defined to have non-negative real parts.

The formula for Ψ_n, Eq. (18), is convenient for estimating Ψ_n when $k_0 R \gg 1$, as we can use the saddle-point method ([16], Chap. 8). There is one relevant saddle point at $s=s_0$ where $s_0 = i(\frac{1}{2}\pi + \Theta)$. As $\cosh s_0 = -\sin \Theta$ and $\sinh(s_0 + i\Theta) = i$, the standard argument gives

$$\Psi_n \sim \frac{1}{\pi i} \mathcal{B}_n(-k_0 \sin \Theta; \beta) e^{ik_0 R} \int \exp\left\{\tfrac{1}{2} i k_0 R (s - s_0)^2\right\} \mathrm{d}s \tag{19}$$

$$\sim \sqrt{\frac{2}{\pi k_0 R}} e^{i(k_0 R - \pi/4)} \mathcal{B}_n(-k_0 \sin \Theta; \beta) \quad \text{as} \quad R \to \infty \tag{20}$$

where the contour of integration in Eq. (19) passes through the saddle point.

When $\beta=0$, we obtain $\mathcal{B}_n(-k_0 \sin \Theta; 0) = i^n e^{ik_0 b \cos \Theta} e^{-in\Theta}$. Then, Eq. (20) agrees with the known far-field expansion of $H_n^{(1)} \times (kr) e^{in\theta}$, when one takes into account that $\theta \sim \pi - \Theta$ and $r \sim R + b \cos \Theta$ as $R \to \infty$.

4.4 Near-Field Behavior of Φ_n. As the expression for Φ_n, Eq. (11), is similar to Eq. (10), it is reasonable to ask if Φ_n corresponds to a simple image term. To see that it does not, let us define polar coordinates centered at the mirror-image point, $(x,y)=(-b,0)$: $x=-b+r' \cos \theta'$, $y=r' \sin \theta'$. Then, calculations similar to those described in the Appendix show that

$$H_n^{(1)}(kr') e^{in(\pi - \theta')} = \frac{(-1)^n}{\pi i} \int_{-\infty}^{\infty + \pi i} e^{kx \sinh \tau} e^{-iky \cosh \tau + kb \sinh \tau - n\tau} \mathrm{d}\tau \tag{21}$$

for $|\theta'| < \pi/2$. The integral on the right-hand side of Eq. (21) should be compared with the integral defining Φ_n, Eq. (11). For them to be equal, the function $A(\tau)$, defined by Eq. (13), would have to be constant: It is not, and it is not well approximated by a nonzero constant. Thus, it is not justified to replace Φ_n with a simple image term: We notice that Fang et al. [2] used image terms similar to those on the left-hand side of Eq. (21), with $\pi - \theta'$ replaced with θ'.

Downloaded 13 Mar 2009 to 138.67.22.171. Redistribution subject to ASME license or copyright; see http://www.asme.org/terms/Terms_Use.cfm

5 Discussion

We have outlined how to solve the scattering problem for a cavity buried in a graded half-space; the result is the infinite linear algebraic system, Eq. (17). The system matrix is very complicated: One has to calculate $(\mathrm{d}/\mathrm{d}r)V_m^n(r)$ at $r=a$, where V_m^n is defined by Eq. (16) as an infinite series of special functions with coefficients given as contour integrals. In principle, the system matrix could be computed but it is unclear whether this is a worthwhile exercise, given the limitations of the underlying model, with both shear modulus and density varying exponentially; see Eq. (1). However, it may be possible to extract asymptotic results from the exact system of equations for small cavities or for cavities that are far from the interface: This remains for future work.

Appendix: Integral Representations

As explained in Sec. 4.1, we need to convert from polar coordinates to Cartesian coordinates in order to apply the interface conditions at $x=0$. This is done using certain integral formulas. Thus, from Ref. [17] (p. 178, Eq. (2)), we have the integral representation

$$H_n^{(1)}(kr) = \frac{1}{\pi i}\int_{-\infty}^{\infty+\pi i} e^{kr\sinh w - nw}\mathrm{d}w \tag{A1}$$

The integration is along any contour in the complex w-plane, starting at $w=-\infty$ and ending at $w=\pi i+\infty$. When $w=\xi+i\eta$, where ξ and η are real, $|e^{kr\sinh w}|=e^{kr\sinh\xi\cos\eta}$. Thus, we can generalize Eq. (A1) to

$$H_n^{(1)}(kr) = \frac{1}{\pi i}\int_{-\infty+i\eta_1}^{\infty+i\eta_2} e^{kr\sinh w - nw}\mathrm{d}w \tag{A2}$$

where the constants η_1 and η_2 must satisfy

$$-\tfrac{1}{2}\pi < \eta_1 < \tfrac{1}{2}\pi \quad \text{and} \quad \tfrac{1}{2}\pi < \eta_2 < \tfrac{3}{2}\pi$$

In other words, we have some flexibility in our choice of contour, flexibility that we shall exploit shortly.

Put $w=\tau+i(\theta-\pi)$. Then Eq. (A2) becomes

$$H_n^{(1)}(kr)e^{in\theta} = \frac{(-1)^n}{\pi i}\int_{-\infty+i\beta_1}^{\infty+i\beta_2} e^{-kr(\sinh\tau\cos\theta+i\cosh\tau\sin\theta)}e^{-n\tau}\mathrm{d}\tau \tag{A3}$$

where the constants β_1 and β_2 must satisfy

$$-\tfrac{1}{2}\pi < \beta_1+\theta-\pi < \tfrac{1}{2}\pi \quad \text{and} \quad \tfrac{1}{2}\pi < \beta_2+\theta-\pi < \tfrac{3}{2}\pi$$

In particular, the choices $\beta_1=0$ and $\beta_2=\pi$ show that

$$H_n^{(1)}(kr)e^{in\theta} = \frac{(-1)^n}{\pi i}\int_{-\infty}^{\infty+\pi i} e^{-kr(\sinh\tau\cos\theta+i\cosh\tau\sin\theta)}e^{-n\tau}\mathrm{d}\tau$$
$$\text{for} \quad \tfrac{1}{2}\pi < \theta < \tfrac{3}{2}\pi \tag{A4}$$

This is the integral representation that we use in Sec. 4.1.

References

[1] Fang, X.-Q., Hu, C., and Du, S. Y., 2006, "Strain Energy Density of a Circular Cavity Buried in Semi-Infinite Functionally Graded Materials Subjected to Shear Waves," Theor. Appl. Fract. Mech., **46**, pp. 166–174.

[2] Fang, X.-Q., Hu, C., and Du, S.-Y., 2007, "Dynamic Stress of a Circular Cavity Buried in a Semi-Infinite Functionally Graded Material Subjected to Shear Waves," ASME J. Appl. Mech., **74**, pp. 916–922.

[3] Fang, X.-Q., Hu, C., and Huang, W.-H., 2007, "Strain Energy Density of a Circular Cavity Buried in a Semi-Infinite Slab of Functionally Graded Materials Subjected to Anti-Plane Shear Waves," Int. J. Solids Struct., **44**, pp. 6987–6998.

[4] Hu, C., Fang, X.-Q., and Huang, W.-H., 2008, "Multiple Scattering of Shear Waves and Dynamic Stress From a Circular Cavity Buried in a Semi-Infinite Slab of Functionally Graded Materials," Eng. Fract. Mech., **75**, pp. 1171–1183.

[5] Hu, C., Fang, X.-Q., and Du, S.-Y., 2007, "Multiple Scattering of Thermal Waves From a Subsurface Spheroid in Exponentially Graded Materials Based on Non-Fourier's Model," Infrared Phys. Technol., **50**, pp. 70–77.

[6] Fang, X. Q., and Hu, C., 2007, "Thermal Waves Scattering by a Subsurface Sphere in a Semi-Infinite Exponentially Graded Material Using Non-Fourier's Model," Thermochim. Acta, **453**, pp. 128–135.

[7] Fang, X.-Q., Hu, C., and Huang, W.-H., 2007, "Dynamic Stress of a Circular Cavity Buried in a Semi-Infinite Functionally Graded Piezoelectric Material Subjected to Shear Waves," Eur. J. Mech. A/Solids, **26**, pp. 1016–1028.

[8] Ursell, F., 1950, "Surface Waves on Deep Water in the Presence of a Submerged Circular Cylinder. I," Proc. Cambridge Philos. Soc., **46**, pp. 141–152.

[9] Gregory, R. D., 1970, "The Propagation of Waves in an Elastic Half-Space Containing a Cylindrical Cavity," Proc. Cambridge Philos. Soc., **67**, pp. 689–710.

[10] Borghi, R., Gori, F., Santarsiero, M., Frezza, F., and Schettini, G., 1996, "Plane-Wave Scattering by a Perfectly Conducting Circular Cylinder Near a Plane Surface: Cylindrical-Wave Approach," J. Opt. Soc. Am. A, **13**, pp. 483–493.

[11] Ting, T. C. T., 1996, *Anisotropic Elasticity*, Oxford University Press, Oxford.

[12] Stevenson, R. C., 1990, "Green's Function for the Helmholtz Equation of a Scalar Wave in an Anisotropic Halfspace," SIAM J. Appl. Math., **50**, pp. 199–215.

[13] Gregory, R. D., 1967, "An Expansion Theorem Applicable to Problems of Wave Propagation in an Elastic Half-Space Containing a Cavity," Proc. Cambridge Philos. Soc., **63**, pp. 1341–1367.

[14] Rangelov, T. V., Manolis, G. D., and Dinerva, P. S., 2005, "Elastodynamic Fundamental Solutions for Certain Families of 2d Inhomogeneous Anisotropic Domains: Basic Derivations," Eur. J. Mech. A/Solids, **24**, pp. 820–836.

[15] Destrade, M., 2007, "Seismic Rayleigh Waves on an Exponentially Graded, Orthotropic Half-Space," Proc. R. Soc. London, Ser. A, **463**, pp. 495–502.

[16] Copson, E. T., 1965, *Asymptotic Expansions*, Cambridge University Press, Cambridge.

[17] Watson, G. N., 1944, *Theory of Bessel Functions*, 2nd ed., Cambridge University Press, Cambridge.

Downloaded 13 Mar 2009 to 138.67.22.171. Redistribution subject to ASME license or copyright; see http://www.asme.org/terms/Terms_Use.cfm